ADVANCES IN NON-FOSTER CIRCUIT AUGMENTED, BROAD BANDWIDTH, METAMATERIAL-INSPIRED, ELECTRICALLY SMALL ANTENNAS

Graduate Student: Ning Zhu
Advisor: Richard W. Ziolkowski

Department of Electrical and Computer Engineering,
The University of Arizona, Tucson, AZ, USA

ABSTRACT

There are always some intrinsic tradeoffs among the performance characteristics: radiation efficiency, directivity, and bandwidth, of electrically small antennas (ESAs). A non-Foster enhanced, broad bandwidth, metamaterial-inspired, electrically small, Egyptian axe dipole (EAD) antenna has been successfully designed and measured to overcome two of these restrictions. By incorporating a non-Foster circuit internally in the near-field resonant parasitic (NFRP) element, the bandwidth of the resulting electrically small antenna was enhanced significantly. The measured results show that the 10 dB bandwidth (BW_{10dB}) of the non-Foster circuit-augmented EAD antenna is more than 6 times the original BW_{10dB} value of the corresponding passive EAD antenna.

Keywords: Broadband antennas, Chu-Thal limit, electrically small antennas, metamaterial-inspired antennas, and non-Foster elements

1. INTRODUCTION

Electrically small antennas (ESAs) have been a topic of great research interest for many years because of their utility for a wide variety of wireless applications. An antenna is electrically small if its electrical size is much smaller than a wavelength at its operational/resonance frequency. However, because of the compact electrical size of ESAs, there are always some tradeoffs among their performance characteristics: radiation efficiency, directivity, and bandwidth. The fundamental bandwidth limitation of an ESA was first derived by Chu [1] and is expressed in terms of the quality factor of the antenna at a simple resonance as:

$$Q_{Chu,lb} = \frac{1}{(ka)^3} + \frac{1}{ka} \tag{1}$$

where a is the radius of the smallest sphere enclosing the entire antenna system and $k=2\pi/\lambda$ (λ is the free-space wavelength). The relation between the upper bound on the half power VSWR

fractional bandwidth and the lower bound on the quality factor, Q_{lb}, is $FBW_{3dB,ub} \approx 2/Q_{lb}$. Taking into account the ESA's radiation efficiency (*RE*) and the differences between the antenna as an effective electric and magnetic dipole radiator [2] - [4], the *Q* lower bound can be further constrained as: $Q_{lb} = RE \times Q_{Chu,lb}$ and $Q_{mag,lb} = 2Q_{elec,lb} = 3Q_{lb}$. In particular, the maximum 3dB bandwidth (BW_{3dB}) for a planar electric antenna is [5], [6] is:

$$BW_{elec,planar} \approx \frac{16}{9\pi} \frac{1}{RE} \left[\frac{(ka)^3}{1+(ka)^2} \right] f_r \qquad (2)$$

where f_r is the resonance frequency of the antenna. Therefore, one observes immediately that there are always tradeoffs among the antenna size (*ka* value), *RE* and bandwidth. Researchers have been successfully approaching the *Q* lower bounds with a variety of passive antenna designs (e.g., [7]). We have successfully designed and measured a variety of metamaterial-inspired electrically small antennas based on electric and magnetic couplings between their driven and near-field resonant parasitic (NFRP) elements to approach the Q_{lb} while maintaining a high *RE* value [7]. Nevertheless, the available instantaneous bandwidth is still restricted by their small electrical size as described by (2).

In order to achieve a broadband ESA, an active non-Foster element has been introduced directly into the NFRP element of the antenna. Being different from traditional external non-Foster matching networks between the antenna and the RF source, our non-Foster circuit is completely incorporated into the antenna and the resulting antenna system is matched to the assumed 50 Ω RF source without any external matching network. The entire system remains based on an electric coupling strategy. This paper reports the experimental results of our non-Foster circuit-augmented Egyptian axe dipole (EAD) antenna design. Note that an approximate 300 MHz operating frequency was selected as the proof-of-concept design reported here.

2. PASSIVE ELECTRIC EGYPTIAN AXE DIPOLE ANTENNA

The original version of the electrically small, planar, EAD antenna was introduced in [8] as the electric component of a Huygens source, an equal combination of an electric and a magnetic dipole. The revised EAD antenna is shown in Figure 1, with $ka = 0.49$ at its resonance frequency. The antenna design is based on the 0.5-oz copper (0.017 mm thick), 31-mil Rogers Duroid™ 5880 ($\varepsilon_r = 2.2$, $\mu_r = 1.0$, loss tangent = 0.0009) board material [9]. The antenna was simulated with the ANSYS/ANSOFT high frequency structure simulator (HFSS). Both the driven (orange object in the front) and NFRP (red object in the back) elements were curved versions of the "I" metamaterial unit cell element introduced in [10]. The driven element is connecting to a 50 Ω RF source, while the NFRP element is working as the real radiating element. Because the electrically small electric dipole is intrinsically capacitive, an ideal 47 nH inductor, connected across a 2.0 mm gap located at the center of NFRP element, provides the majority of the inductance in the whole antenna.

The HFSS simulation results show that the passive antenna is resonating at 298.0 MHz, as shown in Figure 2 (a), with BW_{10dB} = 4.2 MHz. Other characteristics of this EAD antenna were also obtained at resonance frequency from the HFSS simulations: peak gain = 2.21 dB and *RE* = 97.6%. To be more accurate, the quality factor of the EAD antenna was derived with [11, Eq. (96)] and yields: Q-ratio = $Q_{3dB} / Q_{elec,planar} \approx 1.26$, i.e., the ratio of Q_{3dB} to the minimum quality

factor for a planar electric antenna. The radiation pattern is shown in Figure 2 (b). It confirms that the electric EAD antenna radiates as an electrically small electric dipole, i.e., with the standard donut-shaped radiation pattern at the resonance frequency.

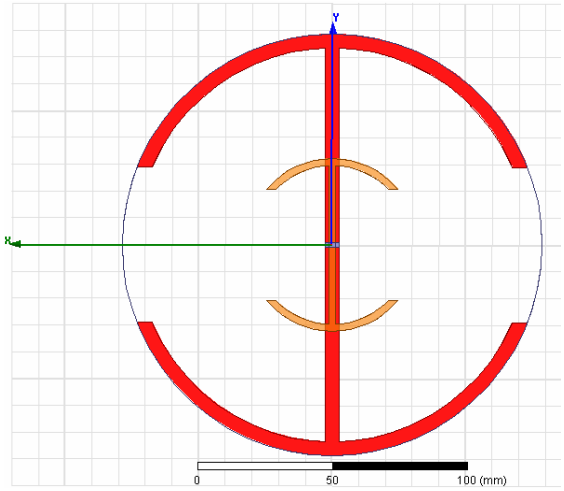

Figure 1. The passive 50 Ω EAD antenna.

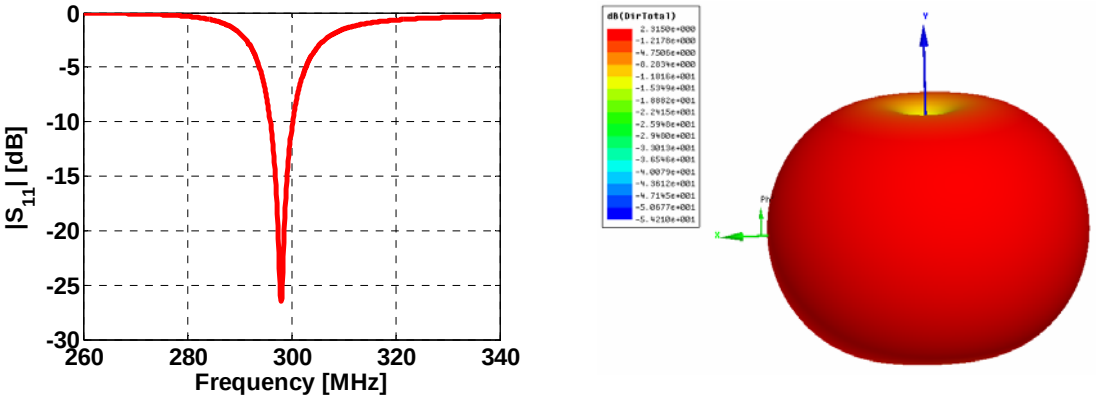

(a) (b)

Figure 2. Simulation results for the 50 Ω EAD antenna with 47 nH inductor. (a) $|S_{11}|$ values; (b) 3D radiation pattern at the 298 MHz resonance frequency.

In order to increase the antenna's bandwidth, the ideal 47 nH inductor was replaced by an ideal, frequency-dependent inductor. It was realized that the passive antenna would become a frequency agile system with the introduction of this frequency-dependent inductance behavior. As shown in Figures 3 (a) and 3 (b), the resonance frequencies varied from 279.3 MHz to 318.5 MHz when the ideal inductor value was swept from 61 nH to 34 nH. Because the ideal inductor value dominates the inductance performance of the whole passive EAD antenna, and resonance frequency $f = (1/2\pi)\ (1/\sqrt{LC})$, where L and C are, respectively, the equivalent inductance and capacitance of the

antenna structure, the resonance frequency increases as the inductor value decreases, i.e., a non-Foster behavior. Figure 3 (b) shows the corresponding inductance curve versus the resonance frequencies.

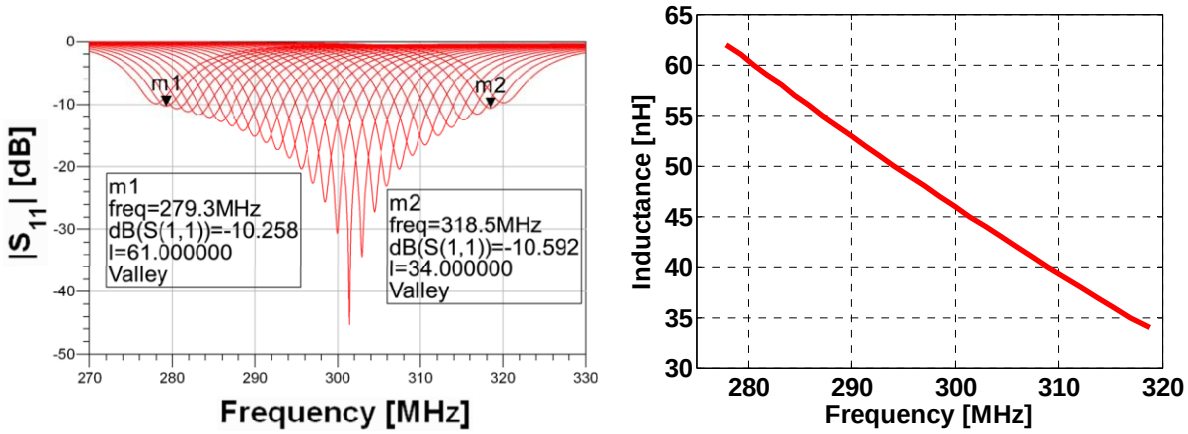

(a) (b)

Figure 3. Frequency agile EAD antenna. (a) Simulated $|S_{11}|$ values, and (b) corresponding inductance versus resonance frequency curve, each point being obtained from the frequency at which $|S_{11}|$ is a minimum in (a) for each inductor value.

3. NON-FOSTER CIRCUIT DESIGN

These frequency agile antenna results inspired the idea to achieve an instantaneous bandwidth by introducing a non-Foster circuit into the antenna system. The Foster reactance theorem, based on positive-definite energy considerations, establishes the fact that the slope of the reactance-frequency curve for any passive system must have a positive slope. Consequently, a reactance-frequency curve with a negative slope, as shown in Figure 3 (b), can only be achieved with an active, non-Foster circuit. As demonstrated in [12] and [13], a non-Foster inductor can be designed to reproduce the inductance-frequency behavior shown in Figure 3 (b). Two practical versions of the original non-Foster circuit configurations [14] were considered for this application: floating and grounded versions. They are shown in Figure 4. One can see that both versions are based on a two-transistor circuit topology. Since the NFRP element of the EAD antenna does not require either of its two metal components to be connected to ground directly, the floating non-Foster circuit was selected for our final non-Foster design. Note that the DC bias circuits for the transistors are omitted in the configurations shown in Figure 4 to simplify their presentation. Note also that the indicated input impedance, Z_{in}, location of the floating design would be connected across the gap of the NFRP element shown in Fig. 1.

The non-Foster circuit was optimized by using the Agilent advanced design system (ADS) to maximally expand its BW_{10dB}. Because there are a variety of lumped element component values that must be included in the ADS optimization process, it was realized that there will always be some tradeoffs between expanding the antenna's bandwidth and decreasing its corresponding $|S_{11}|$ values. The ADS co-simulation results, as shown in Figure 5, verify that approximately 125 MHz

bandwidth, which is a 30 times increase over the passive version, could be achieved. This was found to be true whether ideal lumped elements or commercially available lumped components were taken into account in the designs.

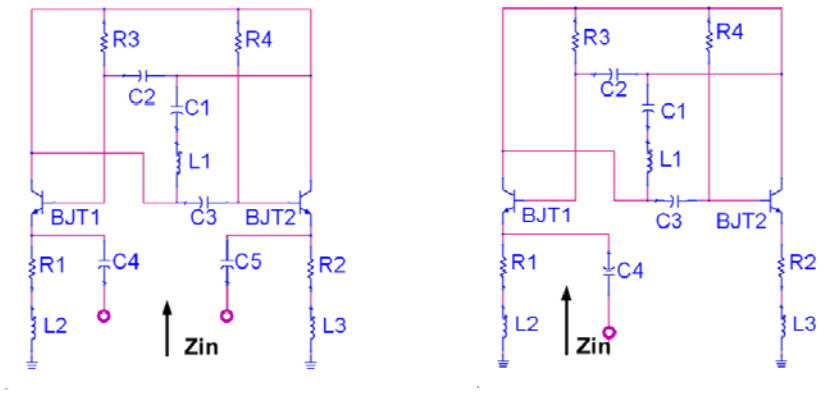

Figure 4. Two non-Foster circuit structures. (a) Floating version, and (b) grounded version.

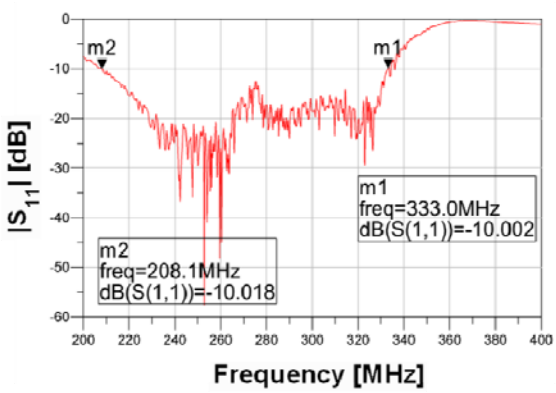

Figure 5. Simulated $|S_{11}|$ values versus the frequency of operation for the EAD antenna augmented with the non-Foster circuit.

4. FABRICATION AND MEASUREMENT

The simulated performance characteristics of the non-Foster augmented EAD antenna demonstrated the very exciting possibility that one could significantly broaden the bandwidth of an electrically small radiating system. A prototype version of the proposed electrically small system was fabricated and measured. However, because of the sensitivity of the highly optimized non-Foster circuits, it proved to be quite difficult to achieve, in practice, the large bandwidths expected from the simulations. In particular, the tolerances of the values of each lumped component used to realize the non-Foster augmented EAD antenna and the parasitic reactances and resistances associated with them, increased the difficulty in tuning the whole active antenna system to obtain satisfactory results. In addition, while the RF stability of the non-Foster circuits was confirmed with ADS Transient simulations, DC stability issues in the prototype experiments

did cause some uncertainty in their initial outcomes. Another simulation-verification issue was found to be the equivalent circuit model of the transistors. The one provided by the vendor was not accurate enough for our applications. The fabricated antenna is shown in Figure 6. One can see the driven and NFRP elements of the EAD antenna, as well as the non-Foster circuit. The largest measured 10dB bandwidth that we achieved experimentally was 25.3 MHz, from 294.1 MHz to 319.4 MHz. The corresponding fractional 10dB bandwidth (FBW_{10dB}) 25.3 MHz / 298 MHz = 8.49% is 6 times more than the corresponding simulated value for the ideal passive EAD antenna, which is 4.2 MHz / 298 MHz = 1.41%.

(a) (b)

Figure 6. Fabricated 300 MHz NIC-augmented EAD antenna. (a) front, and (b) back views.

5. CONCLUSIONS

A broadband, electrically small, non-Foster circuit augmented, EAD antenna was designed and measured around 300 MHz. The measurement results showed that the enhanced FBW_{10dB} was more than 6 times larger than the simulated value of the original passive EAD antenna. Our investigations have also pointed out the need for more accurate passive and active circuit components models for the simulations. Better component values would lead to more satisfactory performance comparisons between the simulated and measured values could be achieved. Additional simulation results, experimental details, and comparisons between the simulated and measured values will be reported in the presentation.

REFERENCES

[1] Chu, L. J., "Physical limitations of omni-directional antennas," Journal of Applied Physics, vol. 19, Dec 1948, 1163-1175.

[2] McLean, J. S., "A re-examination of the fundamental limits on the radiation Q of electrically small antennas," IEEE Transactions on Antennas and Propagation, vol. 44, May 1996, 672-676.

[3] Best, S. R., "Low Q electrically small linear and elliptical polarized spherical dipole Antennas," IEEE Transactions on Antennas and Propagation, vol. 53, Mar. 2005, 1047-1053.

[4] Thal, H. L., "New radiation Q limits for spherical wire antennas," IEEE Transactions on Antennas and Propagation, vol. 54, Oct. 2006, 2757-2763.

[5] Gustafsson, M., Sohl, C. and Kristensson, G., "Illustrations of new physical bounds on linearly polarized antennas," IEEE Transactions on Antennas and Propagation, vol. 57, May 2009, 1319-1327.

[6] Yaghjian, A. D. and Stewart, H. R., "Lower bounds on the Q of electrically small dipole antennas," IEEE Transactions on Antennas and Propagation, vol. 58, Oct. 2010, 3114-3121.
[7] Ziolkowski, R. W., Jin, P. and Lin, C.-C., "Metamaterial-inspired engineering of antennas," Proceedings of the IEEE, vol. 99, Oct. 2011, 1720-1731.
[8] Jin, P. and Ziolkowski, R. W., "Metamaterial-inspired, electrically small, Huygens sources," IEEE Antennas and Wireless Propagation Letters, vol. 9, May 2010, 501-505.
[9] Rogers corporation. http://www.rogerscorp.com/
[10] Ziolkowski, R. W., "Design, fabrication, and testing of double negative metamaterials," IEEE Transactions on Antennas and Propagation, vol. 51, no. 7, July 2003, 1516-1529.
[11] Yaghjian, A. D. and Best, S. R., "Impedance, bandwidth, and Q of antennas," IEEE Transactions on Antennas and Propagation, vol. 53, Apr. 2005, 1298-1324.
[12] Jin, P. and Ziolkowski, R. W., "Broadband, efficient, electrically small metamaterial-inspired antennas facilitated by active near-field resonant parasitic elements," IEEE Transactions on Antennas and Propagation, vol. 58, Feb. 2010, 318-327.
[13] Zhu, N. and Ziolkowski, R. W., "Active metamaterial-inspired broad bandwidth, efficient, electrically small antennas," IEEE Antennas and Wireless Propagation Letters, vol. 10, 2011, 1582-1585.
[14] Linvill, J. G., "Transistor negative-impedance converters," Proceedings of IRE, vol. 41, no. 6, June 1953, 725-729.